FGF21 attenuates hypoxia-induced dysfunction and inflammation in HPAECs via the microRNA-27b-mediated PPARγ pathway

DAN YAO*, QINLIAN HE*, JUNWEI SUN, LUQIONG CAI, JINQIU WEI, GEXIANG CAI, JINGJING LIU, YINUO LIN, LIANGXING WANG and XIAOYING HUANG

Division of Pulmonary Medicine, The First Affiliated Hospital of Wenzhou Medical University, Key Laboratory of Heart and Lung, Wenzhou, Zhejiang 325000, P.R. China

Received November 13, 2020; Accepted April 2, 2021

DOI: 10.3892/ijmm.2021.4949

Abstract. Pulmonary arterial hypertension (PAH), is a chronic and progressive disorder characterized by pulmonary vascular remodeling, including endothelial cell dysfunction and inflammation. MicroRNAs (miRNAs or miRs) play an important role in the development of PAH. In addition, fibroblast growth factor 21 (FGF21) has been found to have marked anti-dysfunction and anti-inflammatory properties. Therefore, the present study aimed to investigate the latent effects of FGF21 against PAH through the miR-27b/peroxisome proliferator-activated receptor γ (PPARγ) axis. Human pulmonary arterial endothelial cells (HPAECs) subjected to hypoxia were used as PAH models. The results revealed that PPARγ expression was downregulated and miR-27b expression was upregulated in the HPAECs exposed to hypoxia. Luciferase assay suggested that PPARγ was a target gene of miR-27b. Furthermore, miR-27b inhibited the expression of the PPARγ gene, thereby aggravating hypoxia-induced HPAEC dysfunction. Moreover, miR-27b activated the nuclear factor-κB signaling pathway and the expression of inflammatory factors [interleukin (IL)-1β, IL-6 and tumor necrosis factor-α] by targeting PPARγ. In addition, the expression of miR-27b decreased following treatment of the hypoxia-exposed HPAECs with FGF21. Furthermore, FGF21 alleviated hypoxia-induced HPAEC dysfunction and inflammation by inhibiting miR-27b expression and thereby promoting PPARγ expression. On the whole, the findings of the present study suggest that FGF21 may serve as a therapeutic target for managing PAH through the miR-27b-mediated PPARγ pathway.

Correspondence to: Professor Xiaoying Huang or Professor Liangxing Wang, Division of Pulmonary Medicine, The First Affiliated Hospital of Wenzhou Medical University, Key Laboratory of Heart and Lung, Nan Baixiang Street, Shangcai Village, Wenzhou, Zhejiang 325000, P.R. China
E-mail: zjwzhxy@126.com
E-mail: wzyxywlx@163.com

*Contributed equally

Key words: fibroblast growth factor 21, human pulmonary arterial endothelial cells, miR-27b, peroxisome proliferator-activated receptor γ, pulmonary arterial hypertension

Introduction

Pulmonary arterial hypertension (PAH) is a chronic and progressive cardiovascular disease with a high mortality rate. It is mainly characterized by pulmonary vascular remodeling, endothelial cell (EC) dysfunction, apoptosis and inflammation. These features increase pulmonary vascular resistance and subsequent pulmonary arterial pressure, causing right heart failure and mortality (1-3). Despite notable improvements being made in therapeutic strategies for PAH, the prognosis of patients with PAH remains unsatisfactory (4). Therefore, a novel signaling pathway related to the pathophysiology of PAH urgently needs to be explored.

Peroxisome proliferator-activated receptor γ (PPARγ) is a nuclear hormone receptor and transcription factor that regulates multiple genes in cardiovascular homeostasis (5). Increasing evidence indicates that PPARγ is a potent, protective regulator of PAH (6) and pulmonary artery ECs (PAECs) (7,8). In addition, a previous study proved that PPARγ activation alleviated hypoxia-induced pulmonary arterial remodeling and collagen deposition in hypoxia-induced PAH (9). However, the role of PPARγ in EC dysfunction and inflammation in hypoxia-exposed human PAECs (HPAECs) has yet to be fully elucidated.

MicroRNAs (miRNAs or miRs) are a conserved class of small non-coding RNAs that can regulate gene expression at the post-transcriptional level (10). Recent studies have indicated that abundant miRNAs participate in the pathogenesis of PAH (11-14). miR-27b has been shown to suppress endothelial cell proliferation and migration in Kawasaki disease (15). In addition, miR-27b has been shown to regulate heat shock protein 90 (Hsp90)/endothelial nitric oxide synthase (eNOS) signaling and nitric oxide production by targeting PPARγ (16). Thus, it was hypothesized that miR-27b is involved in hypoxia-induced HPAEC dysfunction and inflammation.

Fibroblast growth factor 21 (FGF21) is a member of the FGF superfamily, which is mainly expressed in the liver, pancreas, testis and brown adipose tissue. As a hormone, FGF21 regulates a variety of pharmacological effects, including blood glucose and lipid metabolism (17). A previous

study demonstrated that FGF21 attenuated hypoxia-induced dysfunction and apoptosis in HPAECs by alleviating endoplasmic reticulum stress (18). Yu *et al* (19) suggested that FGF21 inhibited macrophage-mediated inflammation by activating nuclear factor erythroid 2-related factor 2 (Nrf2) and suppressing the nuclear factor (NF)-κB signaling pathway. Moreover, a relevant study demonstrated that FGF21 attenuated hypoxia-induced pulmonary hypertension (HPH) by upregulating PPARγ expression and suppressing the expression of inflammatory cytokines (20). Another study reported that FGF21 inhibited miRNA-33 expression to alleviate inflammation and thus prevent atherosclerosis (21), indicating that miRNAs may play an important role in the regulatory effects of FGF21 in several diseases. Therefore, the present study established a model of hypoxia-induced HPAEC to investigate whether FGF21 can alleviate PAH through the miR-27b-mediated PPARγ pathway.

Materials and methods

Reagents and antibodies. Pioglitazone (a PPARγ agonist) was obtained from Sigma-Aldrich; Merck KGaA. FGF21 was obtained from PeproTech, Inc. Rabbit antibodies against PPARγ (cat. no. ab178860) and NF-κB p65 (cat. no. ab32536) were purchased from Abcam). Rabbit antibodies against p-NF-κB (cat. no. 3033T) and β-actin (cat. no. 4970S) were purchased from Cell Signaling Technology, Inc. A horseradish peroxidase (HRP)-conjugated goat anti-rabbit immunoglobulin G (IgG) antibody (cat. no. BL003A) was obtained from Biosharp Life Sciences. Alexa Fluor 488-conjugated donkey anti-rabbit IgG (H+L; cat. no. PC02A) was obtained from Shanghai Boyun BioTech Co., Ltd. Alexa Fluor 594 AffiniPure goat anti-rabbit IgG (H+L; cat. no. 33112ES60) was purchased from Shanghai Yeasen Biotechnology Co., Ltd. Endothelial cell medium (ECM; 1001), fetal bovine serum (FBS) and endothelial cell growth supplement (ECGS) were purchased from ScienCell Research Laboratories, Inc. Phosphate-buffered saline was purchased from HyClone; Cytiva. SuperSignal (R) West Femto Maximum Sensitivity Substrate, radio immunoprecipitation assay (RIPA) buffer, protease and phosphatase inhibitor mini tablets, and the bicinchoninic acid protein assay kit were purchased from Pierce; Thermo Fisher Scientific, Inc. The antifade-4, 6-diamidino-2-phenylindole (DAPI) was purchased from Beijing Solarbio Science & Technology Co., Ltd. The Cell Counting Kit-8 (CCK-8) was purchased from Dojindo Molecular Technologies, Inc. The ELISA kit was purchased from Shanghai Boyun BioTech Co., Ltd.

Cells and cell culture. Primary HPAECs (cat. no. 3100) were obtained from ScienCell Research Laboratories, Inc. For the use of primary cells, the present study was approved by the Ethics Committee of the First Affiliated Hospital of Wenzhou Medical University (Wenzhou, China; approval no. 2020-232). They were cultured in ECM supplemented with 5% FBS, 1% ECGS, 100 μ/ml penicillin and 100 μg/ml streptomycin. After reaching 80-90% confluency, the cells were treated with 0.25% trypsin-ethylene diamine tetraacetic acid (EDTA) for further passaging. Confluent cultures of cells were used in the experiments. For the analysis of the miR-27b/PPARγ axis, the HPAECs were divided into the following groups: i) N, normoxia + negative control (NC) group; ii) H, hypoxia + NC group; iii) H + I, hypoxia + miR-27b inhibitor (100 nM) group; iv) H + I + siPPARγ, hypoxia + miR-27b inhibitor + siPPARγ; v) H + Pio: Hypoxia + pioglitazone (PPARγ agonist, 6.25 μmol/l) + NC group. For the analysis of the FGF21/miR-27b/PPARγ axis, the cells were divided into the following groups: i) N, normoxia + NC group; ii) H, hypoxia + NC group; iii) H + F, hypoxia + FGF21 (50 ng/ml) + NC group; and iv) H + F + m, hypoxia + FGF21 + miR-27b mimic (50 nM) group. The hypoxia-exposed HPAECs were treated as aforementioned for 24 h. The cells in the normoxia group were cultured in a normal incubator (37˚C with 21% O_2, 5% CO_2, and 74% N) for 24 h, while the cells in the hypoxia group were kept in a hypoxia incubator (37˚C with 5% CO_2, 2% O_2, and 90% N_2) for 24 h, with these conditions based on the results of previous studies (18,22).

Cell transfection. The small interfering RNAs (siRNAs) targeting PPARγ (si-PPARγ) with the negative control (si-NC), miRNAs for miR-27b overexpression (miR-27b mimics), respective NC (mimics NC), miR-27b knockdown (miR-27b inhibitors) and respective NC (inhibitors NC) were designed and synthesized by Guangzhou RiboBio Co., Ltd. The Ribo FECT. CP transfection kit (Guangzhou RiboBio Co., Ltd.) was used to transfect the siPPARγ (50 nM), si-NC (50 nM), inhibitor (100 nM), inhibitors NC (100 nM), mimic (50 nM) and mimics NC (50 nM) into the cells following the manufacturer's protocol. Following transfection for 24 h, the cells were used in further experiments.

Western blot analysis. Following treatment, the HPAECs were lysed with ice-cold RIPA lysis buffer containing phenylmethylsulfonyl fluoride (PMSF) for 30 min. The lysates were then centrifuged at 16,000 x g for 30 min at 4˚C, and the supernatant was collected. The protein concentrations were determined using a Pierce bicinchoninic acid (BCA) protein assay kit (Thermo Fisher Scientific, Inc.). Equal amounts of protein (20 μg) were then separated by 10% sodium dodecyl sulfate polyacrylamide gel electrophoresis (SDS-PAGE), transferred onto polyvinylidene fluoride membranes, blocked with 5% skimmed milk for 1 h at room temperature, and incubated overnight with specific primary rabbit antibodies against PPARγ (1:1,000), p-NF-κB (1:1,000), NF-κB p65 (1:1,000) and β-actin (1:1,000) at 4˚C overnight and then incubated with the HRP-labeled secondary antibody (1:10,000) at room temperature for 1 h. β-actin was used as an endogenous control. Super Signal West Fem to Maximum Sensitivity substrate (cat. no. 3409; Shanghai Boyun BioTech Co., Ltd.) was used as the visualization reagent. The optical density of the western blots was quantified using Quantity One 4.6.2 software (Bio-Rad Laboratories, Inc.).

Reverse transcription-quantitative polymerase chain reaction (RT-qPCR). Total RNA was isolated from the treated HPAECs using TRIzol reagent (Sangon Biotech). Reverse transcription was conducted using the Takara PrimeScript kit (cat. no. RR036A; Takara Bio, Inc.) at 37˚C for 15 min. Subsequently, qPCR was performed using the Real-Time PCR System (cat. no. A25742; Thermo Fisher Scientific, Inc.) following the manufacturers' instructions. The PCR amplification reaction were as

follows: 95˚C for 10 min, 95˚C for 15 sec, 62˚C for 30 sec, and 72˚C for 30 sec. Relative quantification was calculated using the $2^{-\Delta\Delta Cq}$ method, as previously described (23). U6 and β-actin were set as internal controls. The primers used for PCR were as follows: miR-27b forward, 5'-GCGCGTTCACAGTGGCTAAG-3' and reverse, 5'-AGTGCAGGGTCCGAGGTATT-3'; interleukin (IL)-1β forward, 5'-CCCTAAACAGATGAAGTGCTCCTT-3' and reverse, 5'-GTAGCTGGATGCCGCCAT-3'; IL-6 forward, 5'-AACCTGAACCTTCCAAAGATGG-3' and reverse, 5'-TCTGGCTTGTTCCTCACTACT-3'; tumor necrosis factor (TNF)-α forward, 5'-CCTCTCTCTAATCAGCCCTCTG-3' and reverse, 5'-GAGGACCTGGGAGTAGATGAG-3'; U6 forward, 5'-AGAGAAGATTAGCATGGCCCCTG-3' and reverse, 5'-ATCCAGTGCAGGGTCCGAGG-3'; and β-actin forward, 5'-CTGGAACGGTGAAGGTGACA-3' and reverse, 5'-AAGGGACTTCCTGTAACAATGCA-3'.

Bioinformatics analysis and dual-luciferase assay. TargetScan (www.targetscan.org) were utilized to predict the binding site between the targeting gene and miR-27b. The 3'-untranslated region (3'-UTR) of PPAR mRNA with the putative/mutant miR-27b-binding site was cloned into the pmiR-RB-Report vector (Guangzhou RiboBio Co., Ltd.). *Renilla* luciferase (Rluc) acted as a reporter and Firefly luciferase (Luc) acted as a control. 293T cells (American Type Culture Collection Co., Ltd.) grown in 96-well plates were co-transfected with the vector (2 μg) and miR-27b mimic (50 nM) using a ribo FECTTM CP transfection kit (Guangzhou RiboBio Co., Ltd.). Following incubation (37˚C with 21% O_2, 5% CO_2, and 74% N) for 48 h, *Renilla* and Firefly luciferase activities were detected using a dual-luciferase reporter assay system (Promega Corporation).

Immunofluorescence (IF). IF assays were conducted to determine the protein expression levels of PPARγ and NF-κB. HPAECs were seeded at a density of $1.0x10^5$ cells per well of a 6-well plate in 2 ml of growth medium. Following stimulation, HPAECs were fixed with 4% paraformaldehyde for 30 min at 37˚C and permeabilized using 0.1% Triton X-100 for 10 min. The cells were then blocked using 5% bovine serum albumin for 30 min at 37˚C and immunostained using anti-PPARγ (1:200) and anti-NF-κB p65 (1:200) antibodies overnight at 4˚C, followed incubation at 24˚C in the dark for 1 h with 1:200 Alexa Fluor 488 conjugated donkey anti-rabbit IgG (H+L) and Alexa Fluor 594 AffiniPure goat anti-rabbit IgG (H+L). For mounting, DAPI was added to the coverslips at 24˚C for 5-10 min. Images were acquired using a fluorescence microscope (Leica DMi8; Leica Microsystems, Inc.). Quantitative analysis was performed using ImageJ analysis software (v 1.51, National Institutes of Health). Each condition was repeated three times per experiment.

Cell viability assay. CCK-8 assay was performed to evaluate the viability of the HPAECs. HPAECs were seeded in 96-well plates at a density of $1x10^4$ cells/well. Following pre-incubation in complete medium at 37˚C in the presence of 21% O_2 and 5% CO_2 for 12-24 h, HPAECs were treated with FGF21, miR-27b mimics, miR-27b inhibitor, siPPARγ and pioglitazone prior to exposure to hypoxia. Following 24 h of exposure to hypoxia, the HPAECs were treated with 10 μl/well CCK-8 reagent at 37˚C for 1 h, and the results were examined every 30 min. The absorbance of each well was measured using a microplate reader (SoftMax®Pro 6 Software) at the wavelength of 450 nm.

Transwell migration chamber assay. Cell migration assay was performed to determine the migration of HPAECs. In the present study, 24-well Transwell system (5 μm; Corning Inc.) was used for migration assays. Subsequently, 600 μl ECM containing 5% FBS were added to the lower chamber to establish a chemical attractant.t HPAECs were suspended in ECM without serum, and 100 μl ($2x10^4$/100 μl) of cell suspension was seeded to the upper chambers of the Transwell plates. Following incubation at 37˚C for 24 h, the cells in the upper chamber were gently wiped off using a cotton swab. The migrated cells were then fixed with 4% paraformaldehyde for 20 min, followed by staining with crystal violet for 20 min at 24˚C. Finally, the migrated cells were counted under a microscope (Leica DMi8, Leica Microsystems, Inc.) by randomly selecting six fields for every sample.

ELISA for the measurement of endothelin-1 (ET-1), TNF-α and IL-1β levels. The levels of accumulated ET-1, TNF-α and IL-1β in the culture medium were determined using ELISA kits (ET-1, cat. no. BP-E10711; IL-1β, cat. no. BP-E10081; IL-6, cat. no. BP-E10140; TNF-α, cat. no. BP-E10110) following the manufacturer's protocol.

Statistical analysis. GraphPad Prism (v7.0; GraphPad Software, Inc.) was used for the statistical analysis of the experimental data. All data are presented as the mean ± SD of at least three independent experiments. The differences among multiple groups were analyzed using one-way ANOVA with repeated measures followed by Tukey's post-hoc test, while differences between two groups were analyzed using an unpaired Student's t-test. $P<0.05$ was considered to indicate a statistically significant difference.

Results

PPARγ expression is downregulated and miR-27b expression is upregulated in HPAECs exposed to hypoxia. HPAECs were cultured under hypoxic conditions for 24 h to examine the changes in PPARγ and miR-27b expression in response to hypoxia. The results of western blot analysis demonstrated that PPARγ expression was significantly decreased in the H group compared with the N group (Fig. 1A). miR-27b expression measured by RT-qPCR was increased in the H group compared with the N group (Fig. 1B). These results indicated that hypoxia decreased PPARγ expression and increased miR-27b expression in HPAECs.

miR-27b supresses PPARγ expression by targeting the PPARγ gene. Based on a bioinformatics database TargetScan, miR-27b was predicted to target PPARγ mRNA (Fig. 1C). Therefore, a luciferase reporter gene assay was performed to examine the direct interaction between PPARγ and miR-27b. The results revealed that miR-27b mimic bound to the PPARγ 3'-UTR compared with miR-27b mimics NC + PPARγ 3'-UTR [NC + wild-type (WT)], markedly inhibiting the fluorescence

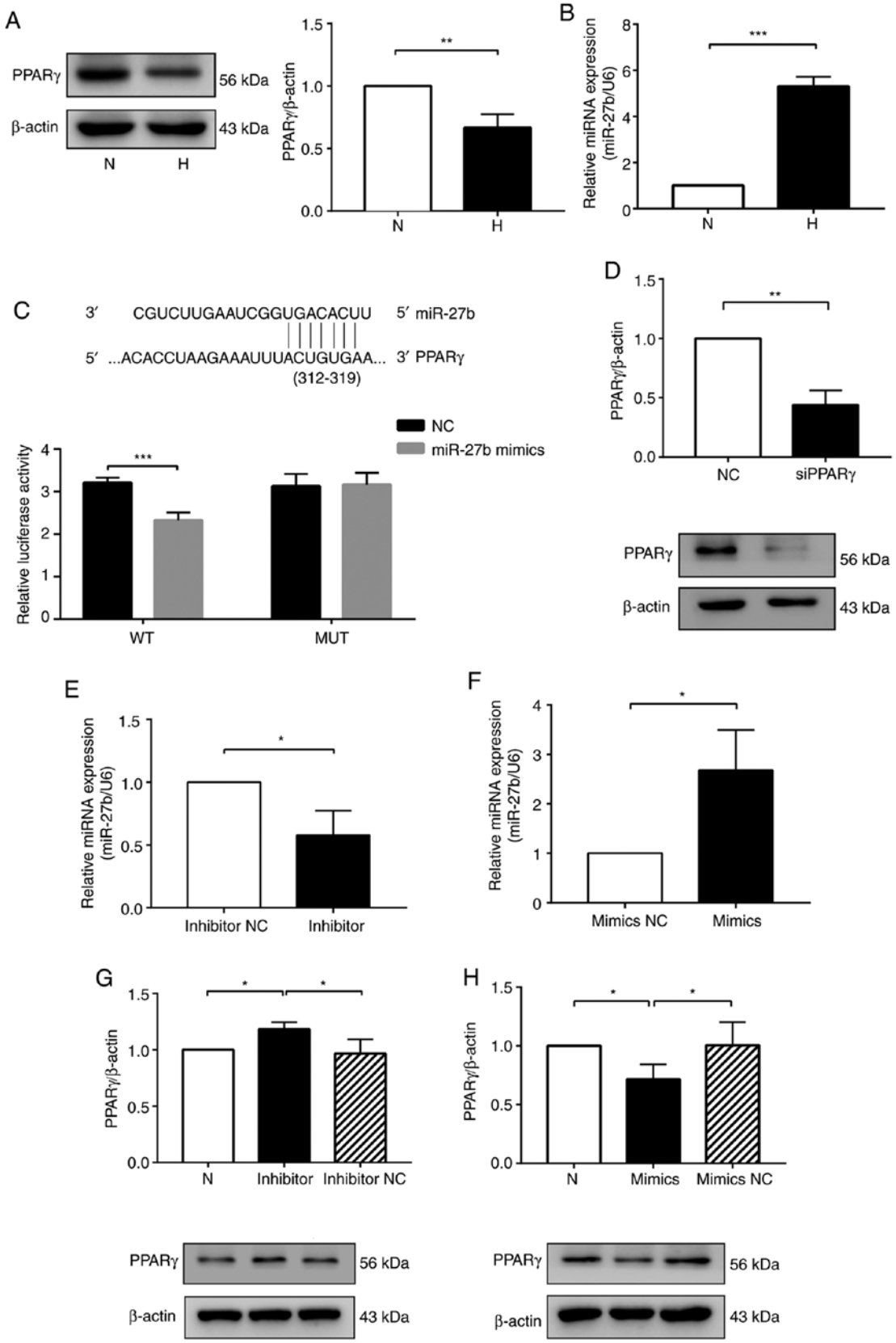

Figure 1. miR-27b suppresses PPARγ expression by targeting the PPARγ gene. (A) Protein expression levels of PPARγ were determined by western blot analysis. (B) Expression of miR-27b was determined by RT-qPCR. (C) Predicted binding sites of miR-27b matching the 3'-UTR of PPARγ. The luciferase activity was decreased following treatment with a combination of miR-27b mimic and PPARγ-3'-UTR-WT, suggesting that miR-27b regulated PPARγ. (D) Western blot analysis to determine PPARγ siRNA efficiency. (E and F) HPAECs were transfected with inhibitors NC or miR-27b inhibitors, mimics NC or miR-27b mimics, and at 24 h following transfection, the expression of miR-27b was determined by RT-qPCR. (G and H) Western blot analysis of PPARγ protein levels in the different groups. β-actin was used as a loading control. The measurement data are presented as the mean ± standard deviation and analyzed by one-way analysis of variance. The experiment was performed in triplicate. *P<0.05; **P<0.01; ***P<0.001, vs. the respective control. RT-qPCR, reverse transcription-quantitative polymerase chain reaction; WT, wild-type; MUT, mutant-type; UTR, untranslated region; NC, negative control; N, normoxia + NC group; H, hypoxia + NC group; PPARγ, peroxisome proliferator-activated receptor γ; HPAECs, human pulmonary arterial endothelial cells.

expression of PPARγ. By contrast, the fluorescence level was unaffected when the cells were co-transfected with the MUT-PPARγ 3'-UTR vector and miR-27b mimic (Fig. 1C). These data thus indicated that miR-27b directly targeted PPARγ by binding to its 3'-UTR.

Subsequently, the present study explored the regulatory effects of miR-27b on PPARγ. PPARγ siRNA was used to downregulate the expression of PPARγ (Fig. 1D). The knockdown of miR-27b was achieved by transfecting the HPAECs with miR-27b inhibitor, and transfection with miR-27b inhibitor markedly reduced miR-27b expression in the HPAECs compared with the inhibitor NC group (Fig. 1E). Moreover, the downregulation of miR-27b markedly promoted the PPARγ protein expression levels in the hypoxia-exposed HPAECs compared with the inhibitor NC group (Fig. 1G). The overexpression of miR-27b was achieved by transfecting HPAECs with miR-27b mimics, and transfection with miR-27b mimics significantly upregulated miR-27b expression in the HPAECs compared with the mimics NC group (Fig. 1F). Simultaneously, the decrease in the PPARγ protein expression levels was detected in the HPAECs overexpressing miR-27b (Fig. 1H).

Furthermore, the results of immunofluorescence staining indicated that the fluorescence intensity of PPARγ was markedly downregulated in the H group compared with the N group. However, the fluorescence intensity of PPARγ was significantly upregulated in the H + I and H + Pio groups compared with the H group. The fluorescence intensity of PPARγ was decreased in the H + I + siPPARγ group compared with the H + I group (Fig. 2A and B). Simultaneously, the results of western blot analysis demonstrated that the protein expression of PPARγ was markedly decreased in the H group compared with the N group. Compared with the H group, the H + I and H + Pio groups exhibited a higher PPARγ level, whereas an opposite trend was observed in the H + I + siPPARγ group (Fig. 2C). Overall, these results illustrated that miR-27b inhibited PPARγ expression via targeting the PPARγ gene.

miR-27b aggravates hypoxia-induced HPAEC dysfunction by targeting PPARγ. Transwell assay was used to determine relative cell numbers and viability so as to assess hypoxia-induced HPAEC cell migratory ability and its regulation by miR-27b. The migratory ability of the HPAECs was decreased in the H group compared with the N group, and was markedly increased in the H + I and H + Pio groups compared with the H group, suggesting that the downregulation of miR-27b and the overexpression of PPARγ had a similar function in repairing the cell migratory ability. However, a significant reduction in the number of migrated cells was observed in the H + I + siPPARγ group compared with the H + I group (Fig. 2D and E). Subsequently, the present study examined the effects of miR-27b on cell viability by CCK-8 assay. As regards the results of cell viability shown in Fig. 2F, the absorbance was reduced in the H group compared with the N group. The absorbance was markedly enhanced in the H + I and H + Pio groups compared with the H group. However, this change was markedly diminished in the H + I + siPPARγ group.

ET-1 is a marker of endothelial dysfunction. The secretion of ET-1 was increased by hypoxia in the H group compared with the N group. ET-1 secretion was significantly decreased in the H + I and H + Pio groups compared with the H group; however, the secretion of ET-1 was upregulated in the H + I + siPPARγ group (Fig. 2G). Hence, these findings suggested that miR-27b exacerbated hypoxia-induced HPAEC dysfunction through the PPARγ gene.

miR-27b enhances hypoxia-induced HPAEC inflammation by targeting PPARγ. The relative levels of p-NF-κB and NF-κB expression in the different groups of HPAECs were determined by western blot analysis to elucidate the molecular mechanisms underlying the effects of miR-27b on PAH-related inflammation. The results revealed that the ratio of p-NF-κB/NF-κB was markedly increased in the H group compared with the N group. The ratio of p-NF-κB/NF-κB was decreased in the H + I and H + Pio groups compared with the H group; however, an adverse trend was observed in the H + I + siPPARγ group (Fig. 3A). The nuclear translocation of NF-κB was then examined by immunofluorescence. The results revealed that hypoxia enhanced the translocation of NF-κB protein into the nucleus, whereas this translocation was inhibited in the H + I and H + Pio groups. However, this inhibitory effect was abolished in the H + I + siPPARγ group (Fig. 3B and C).

Subsequently, the levels of inflammatory factors, such as IL-1β, IL-6 and TNF-α, as secreted cytokines, were examined by ELISA, as this may better reflect their expression in the medium. The results indicated that markedly higher levels of IL-1β, IL-6 and TNF-α were found in the culture medium of HPAECs exposed to hypoxia. The levels of IL-1β, IL-6 and TNF-α were significantly decreased in the H + I and H + Pio groups, whereas this decreasing tendency was reversed in the H + I + siPPARγ (Fig. 3D-F). Similarly, RT-qPCR analysis revealed that the mRNA expression levels of IL-1β, IL-6 and TNF-α in the hypoxia-exposed HPAECs were upregulated in the H group compared with the N group, which was also normalized in the H + I and H + Pio groups. However, the IL-1β, IL-6 and TNF-α expression levels were decreased in the H + I + siPPARγ group (Fig. 3G-I). Taken together, these data suggested that miR-27b promoted hypoxia-induced HPAEC inflammation by targeting PPARγ.

FGF21 attenuates HPAEC dysfunction by inhibiting the miR-27b/PPARγ pathway. The present study then examined the effect of FGF21 on the miR-27/PPARγ axis. Firstly, it was found that the expression of FGF21 was decreased in the H group compared with the N group (Fig. 4A), which indicated that FGF21 may play a protective role in HPH. The results of RT-qPCR indicated that the expression of miR-27b was decreased in the hypoxia-exposed HPAECs following treatment with FGF21 (Fig. 4B). Moreover, the results of immunofluorescence staining revealed that FGF21 significantly increased the fluorescence intensity of PPARγ, which was significantly decreased in the F + m group. (Fig. 4C and D). Consistent with the aforementioned results, western blot analysis revealed that the expression of PPARγ was significantly increased in the H + F group compared with the H group. However, the agonistic effect of FGF21 on PPARγ expression was markedly abolished in the H + F + m group (Fig. 4E). These results indicated

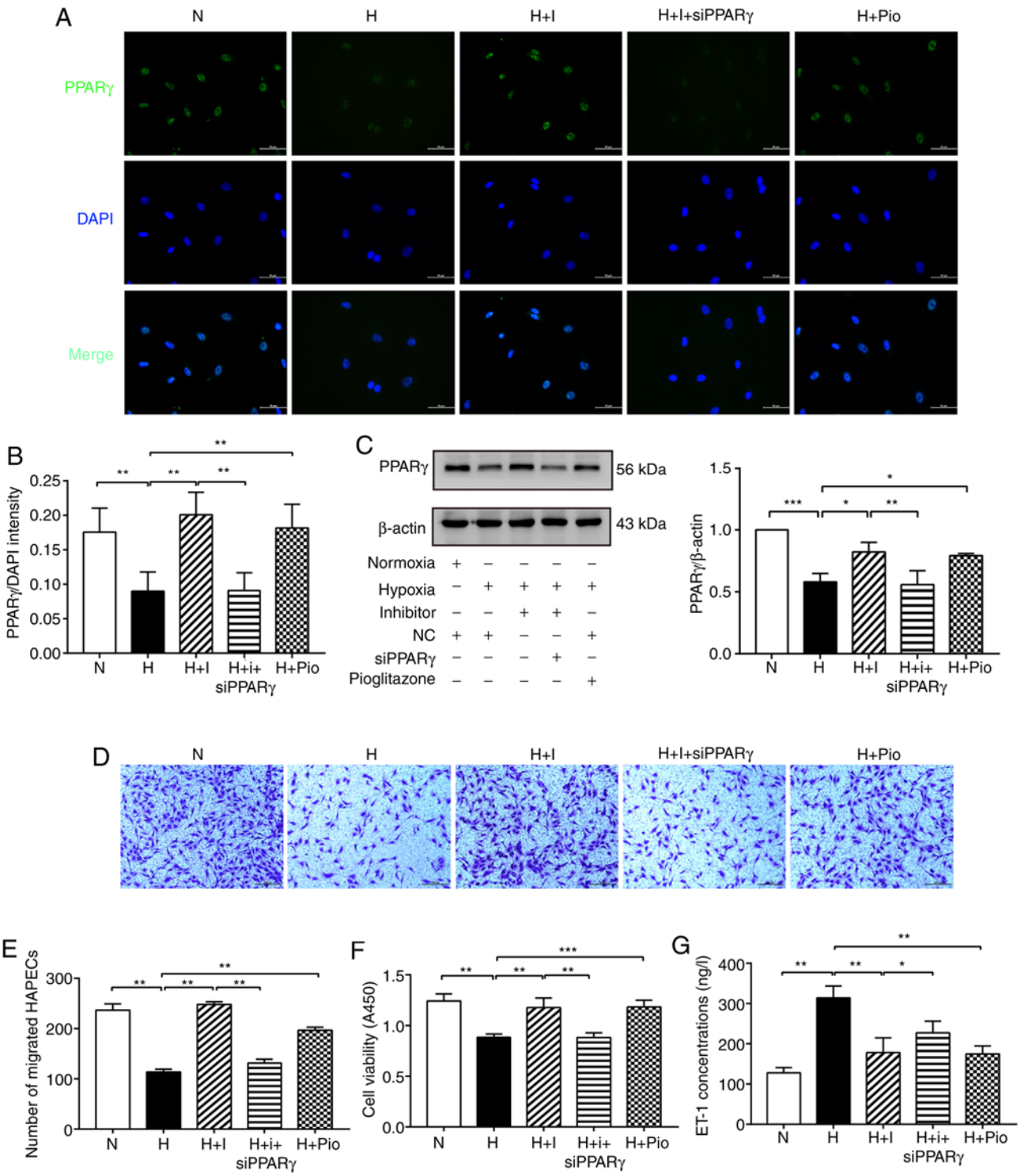

Figure 2. miR-27b aggravates dysfunction of hypoxia-exposed HPAECs by targeting PPARγ. (A and B) Expression of PPARγ (green) was detected by immunofluorescence staining, and the fluorescence intensity of PPARγ was calculated; DAPI was used to stain cell nuclei (blue). Scale bars, 50 μm (magnification, x400). (C) Protein levels of of PPARγ was determined by western blot analysis. β-actin was used as a loading control. (D and E) Cell migration was assessed using Transwell migration chambers. Scale bars, 200 μm (magnification, x100). (F) Cell viability was analyzed by CCK-8 assay. (G) The concentration of ET-1 was assayed by ELISA. The measurement data are presented as mean ± standard deviation and analyzed by one-way analysis of variance. The experiment was performed in triplicate. *P<0.05; **P<0.01; ***P<0.001, vs. the respective control. NC, negative control; N, normoxia + NC group; H, hypoxia + NC group; H + I, hypoxia + miR-27b inhibitor (100 nM) group;) H + I + siPPARγ, hypoxia + miR-27b inhibitor + siPPARγ; H + Pio: Hypoxia + pioglitazone (PPARγ agonist, 6.25 μmol/l) + NC group; DAPI, 4,6-diamidino-2-phenylindole; CCK-8, cell counting kit 8; ELISA, enzyme-linked immunosorbent assay; ET-1, endothelin-1; PPARγ, peroxisome proliferator-activated receptor γ; HPAECs, human pulmonary arterial endothelial cells.

that FGF21 reversed the hypoxia-mediated upregulation of miR-27b, which attenuated the downregulated expression of PPARγ induced by miR-27b overexpression.

Furthermore, CCK-8 and Transwell assays, as well as ELISA were used to examine the effect of FGF21 on the dysfunction of hypoxia-exposed HPAECs via the miR-27b/PPARγ axis.

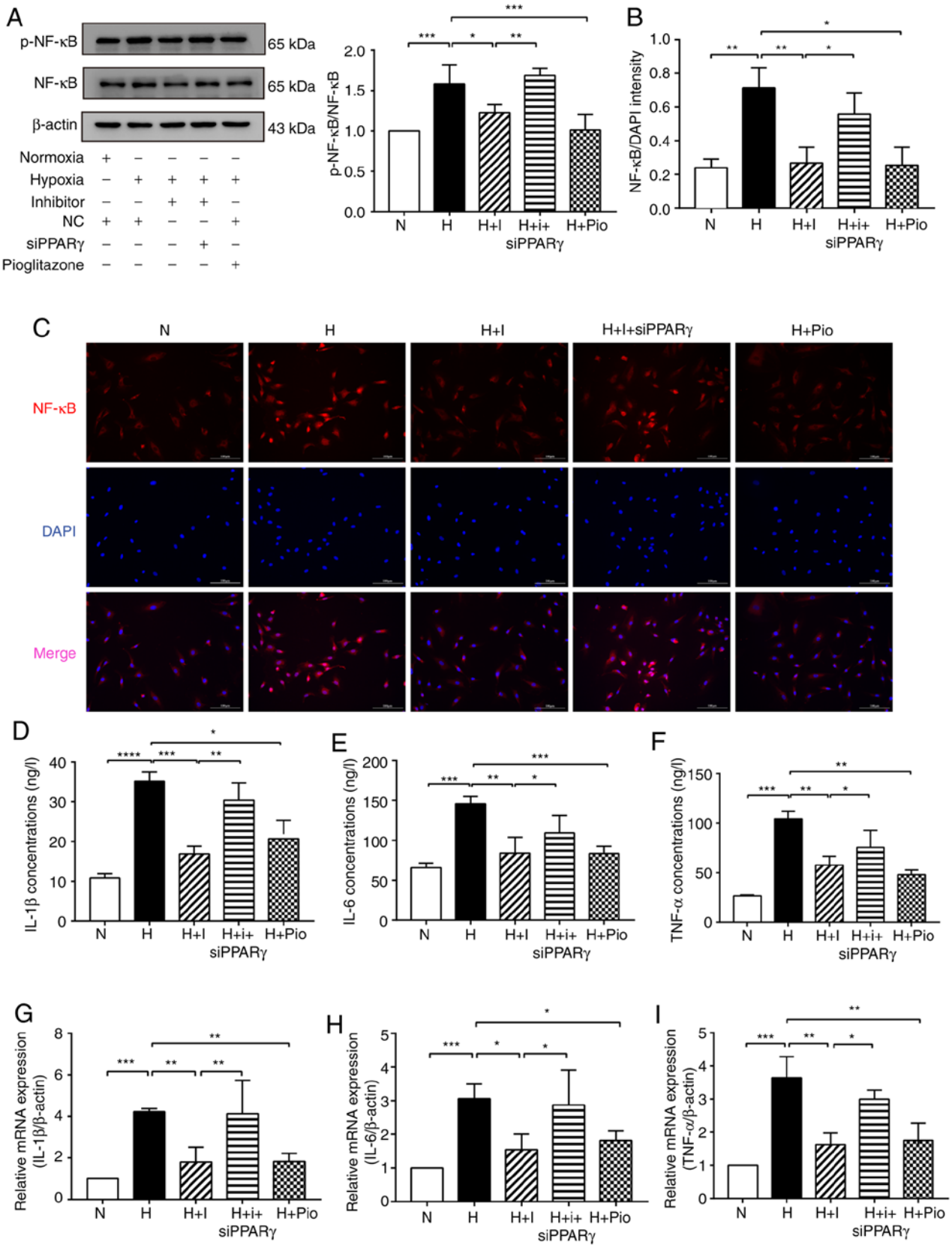

Figure 3. miR-27b pomotes hypoxia-induced HPAEC inflammation by targeting PPARγ. (A) Protein levels of p-NF-κB and NF-κB were detected by western blot analysis. β-actin was used as a loading control. (B and C) Immunofluorescence staining was used to detect NF-κB (red) entering the nucleus. DAPI was used to stain cell nuclei (blue). Scale bars, 100 μm (magnification, x200). (D-F) The expression levels of IL-1β, IL-6 and TNF-α were analyzed using ELISA. (G-I) The expression levels of IL-1β, IL-6 and TNF-α were detected by RT-qPCR. The measurement data are presented as mean ± standard deviation and analyzed using one-way analysis of variance. The experiment was performed in triplicate. *P<0.05; **P<0.01; ***P<0.001, vs. the respective control. NC, negative control; N, normoxia + NC group; H, hypoxia + NC group; H + I, hypoxia + miR-27b inhibitor (100 nM) group;) H + I + siPPARγ, hypoxia + miR-27b inhibitor + siPPARγ; H + Pio: Hypoxia + pioglitazone (PPARγ agonist, 6.25 μmol/l) + NC group; DAPI, 4,6-diamidino-2-phenylindole; ELISA, enzyme-linked immunosorbent assay. RT-qPCR, reverse transcription-quantitative polymerase chain reaction; PPARγ, peroxisome proliferator-activated receptor γ; HPAECs, human pulmonary arterial endothelial cells.

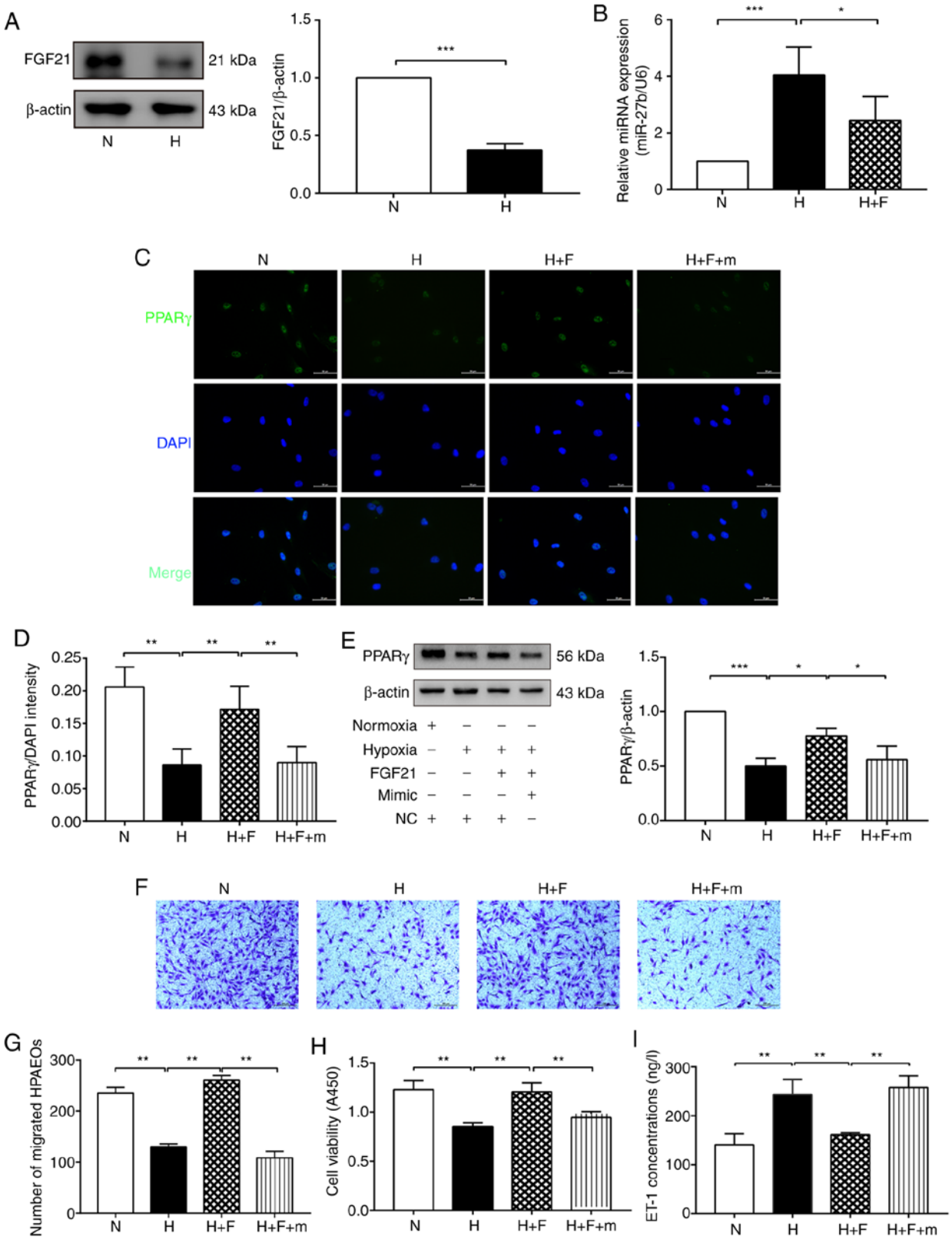

Figure 4. FGF21 attenuates hypoxia-induced dysfunction of HPAECs through the miR-27b/PPARγ axis. (A) Protein levels of of FGF21 was determined by western blot analysis. β-actin was used as a loading control. (B) RT-qPCR was used to determine the expression of miR-27b. (C and D) The expression of PPARγ (green) was detected by immunofluorescence staining, and the fluorescence intensity of PPARγ was calculated. DAPI was used to stain cell nuclei (blue). Scale bars, 50 μm (magnification, x400). (E) Protein levels of of PPARγ was determined by western blot analysis. β-actin was used as a loading control (F and G) Cell migration was assessed using Transwell migration chambers. Scale bars, 200 μm (magnification, x100). (H) Cell viability was analyzed by CCK-8 assay. (I) The concentration of ET-1 was assayed using ELISA. The measurement data were presented as mean ± standard deviation and analyzed using one-way analysis of variance. The experiment was performed in triplicate. *P<0.05; **P<0.01; ***P<0.001, vs. the respective control. N, normoxia + NC group;) H, hypoxia + NC group; H + F, hypoxia + FGF21 (50 ng/ml) + NC group; H + F + m, hypoxia + FGF21 + miR-27b mimic (50 nM) group; RT-qPCR, reverse transcription-quantitative polymerase chain reaction; DAPI, 4,6-diamidino-2-phenylindole; CCK-8, cell counting kit-8; ELISA, enzyme-linked immunosorbent assay; ET-1, endothelin-1; NC, negative control; PPARγ, peroxisome proliferator-activated receptor γ; HPAECs, human pulmonary arterial endothelial cells; FGF21, fibroblast growth factor 21.

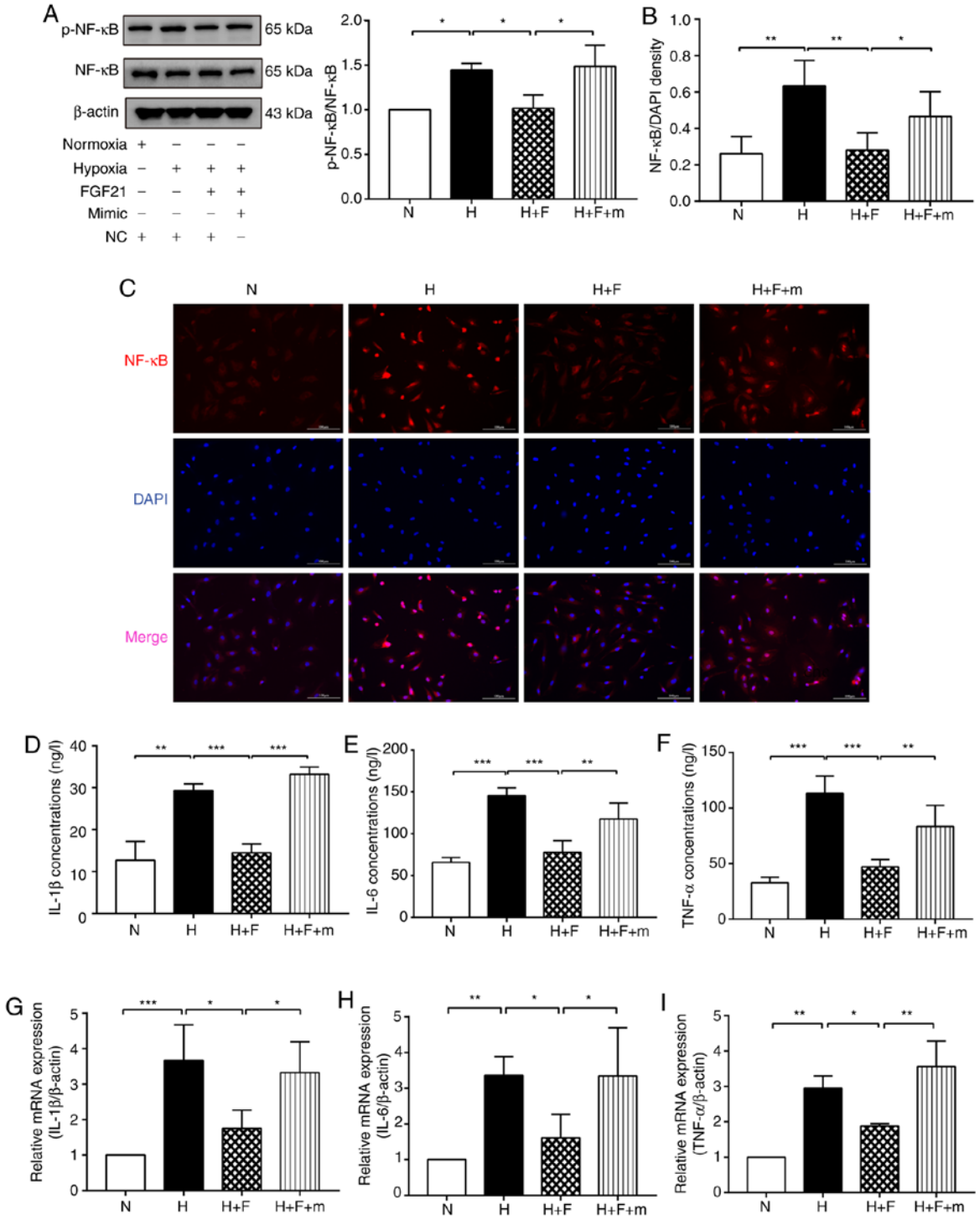

Figure 5. FGF21 suppresses the NF-κB signaling pathway and the inflammatory response in hypoxia-exposed HPAECs via the miR-27b/PPARγ pathway. (A) Protein levels of p-NF-κB and NF-κB were detected by western blot analysis. β-actin was used as a loading control. (B and C) Immunofluorescence staining was used to detect NF-κB (red) entering the nucleus. DAPI was used to stain cell nuclei (blue). Scale bars, 100 μm (magnification, 200). (D-F) The expression levels of IL-1β, IL-6 and TNF-α were analyzed using ELISA. (G-I) The expression levels of IL-1β, IL-6 and TNF-α were detected by RT-qPCR. The measurement data are presented as the mean ± standard deviation and analyzed by one-way analysis of variance. The experiment was performed in triplicate. *P<0.05; **P<0.01; ***P<0.001, vs. the respective control. N, normoxia + NC group;) H, hypoxia + NC group; H + F, hypoxia + FGF21 (50 ng/ml) + NC group; H + F + m, hypoxia + FGF21 + miR-27b mimic (50 nM) group; RT-qPCR, reverse transcription-quantitative polymerase chain reaction; DAPI, 4,6-diamidino-2-phenylindole; ELISA, enzyme-linked immunosorbent assay; NC, negative control; PPARγ, peroxisome proliferator-activated receptor γ; HPAECs, human pulmonary arterial endothelial cells; FGF21, fibroblast growth factor 21.

FGF21 markedly promoted cell viability and migration under hypoxic conditions; however, this change was abolished in the H + F + m group (Fig. 4F-H). As regards ET-1 secretion, the ET-1 level was markedly reduced following FGF21 treatment, whereas the inhibitory effects of FGF21 on ET-1 secretion were reversed in the H + F + m group (Fig. 4I). The aforementioned data illustrated that FGF21 inhibited the expression of miR-27b, thereby promoting PPARγ expression and

consequently alleviating hypoxia-induced HPAEC dysfunction.

FGF21 alleviates hypoxia-induced inflammation in HPAECs through the miR-27b/PPARγ axis. HPAECs were treated with FGF21 prior to exposure to hypoxia to further examine the functional antagonistic effect of FGF21 on hypoxia-induced inflammation. The results of western blot analysis indicated that the ratio of p-NF-κB/NF-κB was markedly decreased in the H + F group compared with the H group. However, this change was reversed in the H + F + m group (Fig. 5A). The results of immunofluorescence staining also revealed that FGF21 inhibited the translocation of NF-κB protein into the nucleus in the hypoxia-exposed HPAECs. However, the inhibitory effects of FGF21 on NF-κB nuclear translocation were abolished in the H + F + m group (Fig. 5B and C). The results of ELISA revealed that FGF21 treatment substantially inhibited the expression of IL-1β, IL-6 and TNF-α in the culture medium of hypoxia-exposed HPAECs, whereas this phenomenon was significantly reversed in the H + F + m group (Fig. 5D-F). Similarly, RT-qPCR analysis revealed that FGF21 reduced the mRNA expression of TNF-α and IL-1β in the hypoxia-exposed HPAECs, whereas this effect was abolished in the H + F + m group (Fig. 5G-I). Collectively, these results demonstrated that FGF21 reversed hypoxia-induced miR-27b upregulation, which attenuated the miR-27b-mediated reduction in PPARγ expression and thereby activated PPARγ to attenuate HPAEC inflammation under hypoxic conditions.

Discussion

PAH is a vascular disorder with a high morbidity and mortality due to the limited treatment methods available. Recent studies have indicated that PAH os closely related to endothelial dysfunction and inflammation (24,25).

Previously, PPARγ was reported to reduce ET-1 and endothelial dysfunction in sickle cell disease-associated PH (SCD-PH) (26). In another study, in a rat model of SU5416/hypoxia (SuHx), oral treatment with the PPARγ agonist, pioglitazone, completely reversed severe PAH and vascular remodeling and prevented right ventricular failure (27). Moreover, PPARγ has been demonstrated to suppress inflammatory cytokine levels in hypoxia-exposed pulmonary artery smooth muscle cells (20). Recently, hypoxia-induced PH was found to be associated with the reductions in PPARγ expression, and the activation of PPARγ attenuated increased pulmonary arterial pressure and right ventricular hypertrophy in hypoxia-exposed mice (9). The aforementioned findings suggest the protective role of PPARγ in PAH. The present study extended these findings by providing evidence that hypoxia decreased PPARγ expression and aggravated HPAEC dysfunction by reducing cell viability and migration ability, and promoting the secretion of ET-1. Moreover, the results indicated that hypoxia activated the NF-κB signaling pathway and increased the expression of inflammatory cytokines. However, all these pathological processes were reversed by treatment with the PPARγ agonist, pioglitazone. These results indicated that PPARγ attenuated endothelial dysfunction and inflammation in hypoxia-exposed HPAECs.

Recently, miR-27b has been suggested to be a key biomarker in various diseases (28-30). miR-27b expression was increased in hypoxia-exposed HPAECs in the present study, indicating that miR-27b was involved in the mechanisms of PAH development. To date, several studies have provided evidence that miR-27b participates in the regulation of inflammatory reactions. For example, Huang *et al* (31) demonstrated that the inhibition of miR-27b attenuated LPS-induced acute lung injure (ALI) via downregulating the NF-κB signaling pathway. In accordance with previous findings (16), the present study found that the downregulated expression of miR-27b enhanced the viability of HPAECs, improved the cell migratory ability and decreased the secretion of ET-1 under hypoxic conditions. The present study found that the downregulated expression of miR-27b ameliorated hypoxia-induced inflammation by inhibiting the expression of NF-κB and inflammatory factors, which was in accordance with previous results (31). A previous study revealed that anti-miR-27b attenuated cardiac hypertrophy and dysfunction in a mouse model of transverse aortic constriction by targeting PPARγ (32). Notably, the present study found that the inhibition of miR-27b reversed the decreased expression of PPARγ in hypoxia-exposed HPAECs by targeting its 3'-UTR. Simultaneously, the effect of miR-27b inhibition on hypoxia-exposed HPAECs was abolished on by transfection with siPPARγ. Taken together, these data indicated that miR-27b promoted hypoxia-exposed HPAEC dysfunction and inflammation via targeting PPARγ.

FGF21, as an important endocrine regulator, has recently been reported to prevent angiotensin II-induced hypertension and vascular dysfunction in mice (33). Previous research has indicated the important roles of FGFs in defining and regulating the functions of some endocrine-relevant tissues and organs, as well as modulating various metabolic processes (34). Apart from its effects on energy metabolism, FGF21 has been shown to exert protective effects against hypertension and vascular dysfunction (35). In the present study, miR-27b was downregulated in hypoxia-exposed HPAECs following FGF21 treatment, suggesting that FGF21 prevented PAH by regulating miR-27b. Based on the aforementioned findings, HPAECs were treated with FGF21 prior to hypoxia exposure to further verify whether FGF21 can protect HPAECs against hypoxia-induced dysfunction via the miR-27b/PPARγ axis. The present study indicated that FGF21 restored EC dysfunction and inhibited the activation of the NF-κB pathway and inflammatory cytokine levels in the hypoxic environment. However, the overexpression of miR-27b blocked the protective effects of FGF21 on the hypoxia-exposed HPAECs. These findings elucidated that FGF21 ameliorated hypoxia-induced HPAEC dysfunction and inflammation via decreasing miR-27b expression, thereby enhancing PPARγ expression. The data further suggested that FGF21 prevented PAH by promoting PPARγ expression.

In conclusion, the findings of the present study suggested that miR-27b exacerbated hypoxia-exposed HPAEC dysfunction and inflammation by inversely regulating PPARγ. However, FGF21 abolished the effect of miR-27b on hypoxia-exposed HPAECs, mainly by inhibiting miR-27b expression, thereby promoting the expression of PPARγ. Due to limited conditions, the role of the FGF21/miR-27b/PPARγ axis *in vivo* remains unclear and the mechanisms through which FGF21 regulates

miR-27b warrants further investigation. Moreover, the effect of the miR-27b/PPARγ axis on the apoptosis of hypoxia-exposed HPAECs needs to be further explored in future studies. Overall, the present study provides theoretical evidence for the basis of further clinical research for the treatment of PAH.

Acknowledgements

Not applicable.

Funding

The present study was supported by the Project of Health Department of Zhejiang Province of China (grant no. 2017171805), the Natural Science Foundation Grants of Zhejiang Province (grant no. Y17H010028), and the Chinese National Natural Science Foundation Grants (grant no. 81873411).

Availability of data and materials

The datasets used and/or analyzed during the current study are available from the corresponding author on reasonable request.

Authors' contributions

DY and QH designed and performed the experiments. QH analyzed the data and wrote the manuscript. XH, LW and YL designed the experiments and assisted in the drafting of the manuscript. JS, LC and JW performed the experiments and collected the data. GC and JL collected the data and performed the analysis. DY and QH confirm the authenticity of all the raw data. All authors have read and approved the final manuscript.

Ethics approval and consent to participate

The present study was approved by the Ethics Committee of the First Affiliated Hospital of Wenzhou Medical University (Wenzhou, China) (approval no. 2020-232).

Patient consent for publication

Not applicable.

Competing interests

The authors declare that they have no competing interests.

References

1. Thompson AAR and Lawrie A: Targeting vascular remodeling to treat pulmonary arterial hypertension. Trends Mol Med 23: 31-45, 2017.
2. Lan NSH, Massam BD, Kulkarni SS and Lang CC: Pulmonary arterial hypertension: Pathophysiology and treatment. Diseases 6: 38, 2018.
3. Rafikova O, Al Ghouleh I and Rafikov R: Focus on early events: Pathogenesis of pulmonary arterial hypertension development. Antioxid Redox Signal 31: 933-953, 2019.
4. Baptista R, Meireles J, Agapito A, Castro G, da Silva AM, Shiang T, Gonçalves F, Robalo-Martins S, Nunes-Diogo A and Reis A: Pulmonary hypertension in Portugal: First data from a nationwide registry. Biomed Res Int 2013: 489574, 2013.
5. Pelham CJ, Ketsawatsomkron P, Groh S, Grobe JL, de Lange WJ, Ibeawuchi SR, Keen HL, Weatherford ET, Faraci FM and Sigmund CD: Cullin-3 regulates vascular smooth muscle function and arterial blood pressure via PPARγ and RhoA/Rho-kinase. Cell Metab 16: 462-472, 2012.
6. Hansmann G and Zamanian RT: PPARgamma activation: A potential treatment for pulmonary hypertension. Sci Transl Med 1: 12ps14, 2009.
7. Diebold I, Hennigs JK, Miyagawa K, Li CG, Nickel NP, Kaschwich M, Cao A, Wang L, Reddy S, Chen PI, *et al*: BMPR2 preserves mitochondrial function and DNA during reoxygenation to promote endothelial cell survival and reverse pulmonary hypertension. Cell Metab 21: 596-608, 2015.
8. Archer SL, Marsboom G, Kim GH, Zhang HJ, Toth PT, Svensson EC, Dyck JR, Gomberg-Maitland M, Thébaud B, Husain AN, *et al*: Epigenetic attenuation of mitochondrial superoxide dismutase 2 in pulmonary arterial hypertension: A basis for excessive cell proliferation and a new therapeutic target. Circulation 121: 2661-2671, 2010.
9. Cai G, Liu J, Wang M, Su L, Cai M, Huang K, Li X, Li M, Wang L and Huang X: Mutual promotion of FGF21 and PPARγ attenuates hypoxia-induced pulmonary hypertension. Exp Biol Med (Maywood) 244: 252-261, 2019.
10. Small EM and Olson EN: Pervasive roles of microRNAs in cardiovascular biology. Nature 469: 336-342, 2011.
11. Tan H, Yao H, Lie Z, Chen G, Lin S and Zhang Y: MicroRNA-30a-5p promotes proliferation and inhibits apoptosis of human pulmonary artery endothelial cells under hypoxia by targeting YKL-40. Mol Med Rep 20: 236-244, 2019.
12. Zhao H, Guo Y, Sun Y, Zhang N and Wang X: miR-181a/b-5p ameliorates inflammatory response in monocrotaline-induced pulmonary arterial hypertension by targeting endocan. J Cell Physiol 235: 4422-4433, 2020.
13. Zhao M, Chen N, Li X, Lin L and Chen X: MiR-19a modulates hypoxia-mediated cell proliferation and migration via repressing PTEN in human pulmonary arterial smooth muscle. Life Sci 239: 116928, 2019.
14. Mondejar-Parreño G, Callejo M, Barreira B, Morales-Cano D, Esquivel-Ruiz S, Filice M, Moreno L, Cogolludo A and Perez-Vizcaino F: miR-1 induces endothelial dysfunction in rat pulmonary arteries. J Physiol Biochem 75: 519-529, 2019.
15. Rong X, Ge D, Shen D, Chen X, Wang X, Zhang L, Jia C, Zeng J, He Y, Qiu H, *et al*: miR-27b suppresses endothelial cell proliferation and migration by targeting Smad7 in kawasaki disease. Cell Physiol Biochem 48: 1804-1814, 2018.
16. Bi R, Bao C, Jiang L, Liu H, Yang Y, Mei J and Ding F: MicroRNA-27b plays a role in pulmonary arterial hypertension by modulating peroxisome proliferator-activated receptor γ dependent Hsp90-eNOS signaling and nitric oxide production. Biochem Biophys Res Commun 460: 469-475, 2015.
17. Geng L, Lam KSL and Xu A: The therapeutic potential of FGF21 in metabolic diseases: From bench to clinic. Nat Rev Endocrinol 16: 654-667, 2020.
18. Chen A, Liu J, Zhu J, Wang X, Xu Z, Cui Z, Yao D, Huang Z, Xu M, Chen M, *et al*: FGF21 attenuates hypoxia-induced dysfunction and apoptosis in HPAECs through alleviating endoplasmic reticulum stress. Int J Mol Med 42: 1684-1694, 2018.
19. Yu Y, He J, Li S, Song L, Guo X, Yao W, Zou D, Gao X, Liu Y, Bai F, *et al*: Fibroblast growth factor 21 (FGF21) inhibits macrophage-mediated inflammation by activating Nrf2 and suppressing the NF-κB signaling pathway. Int Immunopharmacol 38: 144-152, 2016.
20. Liu J, Cai G, Li M, Fan S, Yao B, Ping W, Huang Z, Cai H, Dai Y, Wang L and Huang X: Fibroblast growth factor 21 attenuates hypoxia-induced pulmonary hypertension by upregulating PPARγ expression and suppressing inflammatory cytokine levels. Biochem Biophys Res Commun 504: 478-484, 2018.
21. Guo Y, Luo F, Yi Y and Xu D: Fibroblast growth factor 21 potentially inhibits microRNA-33 expression to affect macrophage actions. Lipids Health Dis 15: 208, 2016.
22. Huang X, Mao W, Zhang T, Wang M, Wang X, Li Y, Zhang L, Yao D, Cai X and Wang L: Baicalin promotes apoptosis and inhibits proliferation and migration of hypoxia-induced pulmonary artery smooth muscle cells by up-regulating A2a receptor via the SDF-1/CXCR4 signaling pathway. BMC Complement Altern Med 18: 330, 2018.
23. Livak KJ and Schmittgen TD: Analysis of relative gene expression data using real-time quantitative PCR and the 2(-Delta Delta C(T)) method. Methods 25: 402-408, 2001.

24. Cao Y, Zhang X, Wang L, Yang Q, Ma Q, Xu J, Wang J, Kovacs L, Ayon RJ, Liu Z, *et al*: PFKFB3-mediated endothelial glycolysis promotes pulmonary hypertension. Proc Natl Acad Sci USA 116: 13394-13403, 2019.
25. Ban Y, Liu Y, Li Y, Zhang Y, Xiao L, Gu Y, Chen S, Zhao B, Chen C and Wang N: S-nitrosation impairs KLF4 activity and instigates endothelial dysfunction in pulmonary arterial hypertension. Redox Biol 21: 101099, 2019.
26. Kang BY, Park K, Kleinhenz JM, Murphy TC, Sutliff RL, Archer D and Hart CM: Peroxisome proliferator-activated receptor γ regulates the V-Ets avian erythroblastosis virus E26 oncogene homolog 1/microRNA-27a axis to reduce endothelin-1 and endothelial dysfunction in the sickle cell mouse lung. Am J Respir Cell Mol Biol 56: 131-144, 2017.
27. Legchenko E, Chouvarine P, Borchert P, Fernandez-Gonzalez A, Snay E, Meier M, Maegel L, Mitsialis SA, Rog-Zielinska EA, Kourembanas S, *et al*: PPARγ agonist pioglitazone reverses pulmonary hypertension and prevents right heart failure via fatty acid oxidation. Sci Transl Med 10: eaao0303, 2018.
28. Hannafon BN, Cai A, Calloway CL, Xu YF, Zhang R, Fung KM and Ding WQ: miR-23b and miR-27b are oncogenic microRNAs in breast cancer: Evidence from a CRISPR/Cas9 deletion study. BMC Cancer 19: 642, 2019.
29. Yang X, Chen J, Liao Y, Huang L, Wen C, Lin M, Li W, Zhu Y, Wu X, Iwamoto A, *et al*: MiR-27b-3p promotes migration and invasion in colorectal cancer cells by targeting HOXA10. Biosci Rep 39: BSR20191087, 2019.
30. Chen J, Wang Y, Du G, Zhang W, Cao T, Shi L, Wang Y, Mi J and Tang G: Down-regulation of miRNA-27b-3p suppresses keratinocytes apoptosis in oral lichen planus. J Cell Mol Med 23: 4326-4337, 2019.
31. Huang Y, Huang L, Zhu G, Pei Z and Zhang W: Downregulated microRNA-27b attenuates lipopolysaccharide-induced acute lung injury via activation of NF-E2-related factor 2 and inhibition of nuclear factor κB signaling pathway. J Cell Physiol 234: 6023-6032, 2019.
32. Wang J, Song Y, Zhang Y, Xiao H, Sun Q, Hou N, Guo S, Wang Y, Fan K, Zhan D, *et al*: Cardiomyocyte overexpression of miR-27b induces cardiac hypertrophy and dysfunction in mice. Cell Res 22: 516-527, 2012.
33. Pan X, Shao Y, Wu F, Wang Y, Xiong R, Zheng J, Tian H, Wang B, Wang Y, Zhang Y, *et al*: FGF21 prevents angiotensin II-induced hypertension and vascular dysfunction by activation of ACE2/angiotensin-(1-7) axis in mice. Cell Metab 27: 1323-1337.e5, 2018.
34. Kharitonenkov A, Shiyanova TL, Koester A, Ford AM, Micanovic R, Galbreath EJ, Sandusky GE, Hammond LJ, Moyers JS, Owens RA, *et al*: FGF-21 as a novel metabolic regulator. J Clin Invest 115: 1627-1635, 2005.
35. Ruan CC, Kong LR, Chen XH, Ma Y, Pan XX, Zhang ZB and Gao PJ: A_{2A} receptor activation attenuates hypertensive cardiac remodeling via promoting brown adipose tissue-derived FGF21. Cell Metab 28: 476-489.e5, 2018.